(Received 22 October 2023, Accepted 18 January 2024, Scheduled 1 February 2024)

Calculation and Optimization of Magnetic Leakage in Electric Vehicle WPT Based on Bidirectional Inverse Series Coils of Four Meshes

Xueyi Zhang[1], Bin Li[1], Liquan Ren[1], Pengsheng Kong[3], and Zhongqi Li[1, 2, 3, *]

[1] *College of Electrical and Information Engineering, Hunan University of Technology, Zhuzhou 412007, China*
[2] *College of Electrical and Information Engineering, Hunan University, Changsha 410013, China*
[3] *College of Railway Transportation, Hunan University of Technology, Zhuzhou 412007, China*

ABSTRACT: In the wireless power transfer (WPT) system of electric vehicles, the system leakage magnetic field and transmission efficiency depend on the coil structure, and the traditional unipolar coil has high transmission efficiency but generates high leakage magnetic field. In order to maintain the transmission efficiency while reducing the magnetic leakage and improve the safety index of the WPT system, this paper proposes a bidirectional inverse series coil of four meshes structure (FBISC), which maintains the high transmission efficiency of the WPT system only by the advantages of the coil structure without applying any metal materials and shielding coils. At the same time, the leakage field produced by the coil structure of the target area is less than the safety limit value, which makes the traditional shielding coils no longer necessary, and is light, clean, and highly efficient. First, the leakage magnetic field generated by the coil in the target region after energization is analytically calculated using a vector potential-based method for calculating the magnetic induction strength of rectangular coils. Secondly, a coil parameter assignment optimization method that weighs two structural performance indexes, namely, transmission efficiency and leakage magnetic field, is given to obtain the coil parameters that satisfy the given conditions. Furthermore, the proposed coil structure is compared with the conventional coil structure. Compared with the conventional unipolar coil, the bidirectional inverse series coil of four meshes reduces the leakage magnetic field by 56.4% and sacrifices only 2.38% of the transmission efficiency. Compared with the reverse double D coil (DD coil), the bidirectional inverse series coils of four meshes reduces the leakage magnetic field in the target region by 48.5% and sacrifices only 1.3% of the transmission efficiency. Finally, an electric vehicle WPT system with shielding is built to verify the correctness of the proposed structure. The results show that the leakage magnetic field of the FBISC coil structure in the target region is only 5.22 μT, and the transmission efficiency is more than 95% at an output power of 4 kW.

1. INTRODUCTION

The rapid development of today's industry has put forward higher requirements for the energy technology industry. In order to realize the strategic goal of green, low-carbon and high-efficiency energy, wireless power transfer technology has emerged. Magnetic Coupling Resonant Wireless Power Transfer (MCRWPT) is a technology that has significant advantages such as convenient charging, safety, and high degree of freedom, and is widely used in electric vehicles, rail transportation, medical devices, portable electronic products, and other fields [1–4]. This technology has produced far-reaching changes in the field of electrical charging, making the transition from wired to wireless and breaking the boundaries of traditional wired charging. However, at the same time, as the charging power increases, the leakage magnetic field of the traditional unipolar coil also increases, which can jeopardize the safety of the users [5, 6]. Therefore, in order to reduce the leakage magnetic field of WPT systems, three types of typical shielding methods are usually used: passive shielding, reactive resonance shielding, and active shielding.

Passive shielding can be divided into three categories through the shielding method: ferromagnetic core shielding, non-ferromagnetic metal shielding, and electromagnetic superconducting material shielding.

Ferrite is mainly used as a shielding material in ferromagnetic core shielding, which has advantages of high resistivity, easy magnetization, and it is suitable for high-frequency field. The traditional ferrite material, which is brittle, having poor mechanical properties, is not usable in this scenario, and finding new shielding materials adapted to the high-frequency environment has become a new goal for scholars. Long T team at the University of Cambridge, UK, took the lead in the application of nanocrystals in magnetic core shielding research [7]. However, it was found that the eddy current loss and high conductivity of nanocrystals led to the addition of extra losses in the system, which in turn reduced the transmission efficiency of the whole system, and thus were not enough to completely replace ferrite materials. Nanocrystals have good magnetic properties but poor energy efficiency performance, and ferrite has poor magnetic properties but good energy efficiency, so there is a complementary relationship between these two materials. Based on this, [8] proposes a core shielding method combining

* Corresponding author: Zhongqi Li (my3eee@126.com).

nanocrystals and ferrite, and the effectiveness of the proposed method is verified by experiment and simulation.

Non-ferromagnetic metal shielding uses non-ferromagnetic metal materials to suppress the high-frequency alternating leakage electromagnetic field generated by the coupling coil. The Hebei University of Technology team used aluminum and copper materials to apply shielding to the WPT system, and the study showed that the shielding performance of aluminum and copper materials is related to its position, and the shielding effect is better when the metal plate is located in the middle of the transmitter-receiver coil and close to the receiver coil [9]. Zhu's team which come from the Chinese Academy of Sciences did some research on the impact of aluminum shielding plate in the WPT system, and they found that the whole aluminum plate has a good shielding effect, but reduces the power density of the system, which will produce a lot of eddy current losses [10].

Electromagnetic superconducting material is a new type of artificial composite material with excellent performance in magnetic field regulation, which can be used for leakage shielding in WPT system [11]. A large number of studies have shown that superconducting material shielding can improve the shielding and transmission performance of the system, but the placement requirements are strict, limiting the flexibility of the WPT system to be used in practical applications [12–16].

The shielding of reactive resonance can be used for WPT system. Reactive resonant shielding uses reactive resonant coils to suppress the high-frequency alternating magnetic field generated in WPT systems, mainly through the leakage of magnetic field generated in the shielding coil to offset the original magnetic field to achieve the shielding effect [17–19]. The Korea Advanced Institute of Science and Technology (KAIST) team has achieved this by tuning the capacitor reactive shielding method to cancel the magnetic field at a specific efficiency [20]. However, the design of parameters and capacitance is demanding, and the control method is complex.

Active shielding is achieved by applying additional excitation or inverting the shielding coil in series above the main coil to generate a reverse canceling magnetic field. Ref. [21] proposed a double-loop active shielding coil directly connected in series with the primary coil to reduce the leakage level of the WPT system, while realizing additional coupling decoupling between the shielding and the receiving coil, but the structure is complicated, which affects the coupling performance between the receiving and transmitting coils. Lee and other scholars, from the Korea Advanced Institute of Science and Technology (KAIST), proposed a novel hybrid loop array structure that combines a shielding coil and an amplifying coil. In this structure, the shielding coil reduces the leakage field strength, and the amplifying coil enhances the magnetic field strength between the coupling coils, but the additional shielding coil also further increases the size of the system and sacrifices the high transmission efficiency [22]. However, the additional shielding coils further increase the size of the system and sacrifice the high transmission efficiency.

In this paper, a four bidirectional inverse series coil of four meshes for electric vehicle wireless charging system is proposed. This structure is the main component of the WPT system, maintains the high transmission efficiency of the system through the structural advantages of the main coil alone, without the application of any metallic materials and shielding coils, and keeps the leakage magnetic field in the target area below the safety limit, making the conventional shielding coils unnecessary. Its receiving and transmitting coils are identical, and both consist of four coil units of the same size and number of turns, each of which is connected in reverse series with neighboring coils in both the transverse and longitudinal directions. The structure improves the safety index during electric vehicle charging and maintains a high transmission efficiency. This paper analyzes the shielding principle of the bidirectional inverse series coils of four meshes and proposes a coil parameter assignment optimization method to trade off the transmission efficiency and shielding effect. Finally, the rationality of the proposed structure is verified through theoretical calculation, simulation, and experiment.

2. FBISC STRUCTURE

2.1. Calculation of Coil Magnetic Induction

In this paper, the method of calculating the magnetic induction strength of a rectangular coil based on vector magnetic potential mentioned in the literature [23, 24] is used to calculate the magnetic induction strength generated by the coil in the target region. The calculation method is described as follows in relation to the coil structure mentioned in this paper.

Figure 1 shows a set of coil cells. Coil_1 length-width is denoted as a_1, a_2; Coil_2 length-width is denoted as b_1, b_2; O_1 and O_2 are the centers of the two coil cells, and the perpendicular distance between them is denoted as h. Let an arbitrary point P (x, y, z) in the space of Figure 1, and its vector magnetic potential expression is as follows:

$$\vec{A}(x,y,z) = \frac{\mu_0}{4\pi}\int_v \frac{\vec{J}(x',y',z')\,dv'}{\vec{R}} \tag{1}$$

where $\vec{J}$ denotes the current density, and v denotes the current distribution in Coil_1. Based on the vector magnetic potential, the expression for the magnetic induction $\vec{B}$ can be obtained as:

$$\vec{B} = \nabla \times \vec{A} = \left(\frac{\partial A_z}{\partial y} - \frac{\partial A_y}{\partial z}\right)\vec{a_x} + \left(\frac{\partial A_x}{\partial z} - \frac{\partial A_z}{\partial y}\right)\vec{a_y} + \left(\frac{\partial A_y}{\partial x} - \frac{\partial A_x}{\partial y}\right)\vec{a_z} \tag{2}$$

where A_x, A_y, and A_z are represented as the components of the vector magnetic potential $\vec{A}$ in the X-axis, Y-axis, and Z-axis, respectively. According to the method of calculating the magnetic induction strength of a rectangular coil based on the vector magnetic potential, the magnetic induction strength components of a single coil in the X-axis, Y-axis, and Z-axis can be obtained

$$\dot{B}_x = \frac{1}{4\pi^2}\int_{-\infty}^{\infty}\int_{-\infty}^{\infty}\frac{-j2\mu_0 I\sin(\xi a_1)\sin(\eta a_2)}{\eta}$$

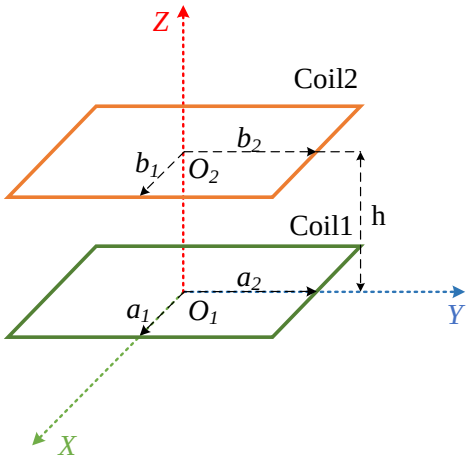

FIGURE 1. Schematic diagram of coil unit.

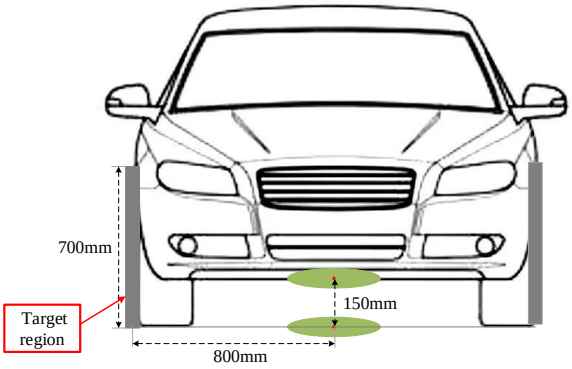

FIGURE 2. Target region of electric vehicles.

$$\cdot e^{s_1 k} \cdot e^{-kz} \cdot e^{\mathrm{j}(x\xi+y\eta)} d\xi d\eta \tag{3}$$

$$\dot{B}_y = \frac{1}{4\pi^2} \int_{-\infty}^{\infty} \int_{-\infty}^{\infty} \frac{-j2\mu_0 I \sin(\xi a_1) \sin(\eta a_2)}{\xi}$$

$$\cdot e^{s_1 k} \cdot e^{-kz} \cdot e^{\mathrm{j}(x\xi+y\eta)} d\xi d\eta \tag{4}$$

$$\dot{B}_z = \frac{1}{4\pi^2} \int_{-\infty}^{\infty} \int_{-\infty}^{\infty} \frac{-2\mu_0 Ik \sin(\xi a_1) \sin(\eta a_2)}{\xi\eta}$$

$$\cdot e^{s_1 k} \cdot e^{-kz} \cdot e^{\mathrm{j}(x\xi+y\eta)} d\xi d\eta \tag{5}$$

where ξ and η are the double Fourier integral variables; I is the current flowing through the coil; and the total magnetic induction of a single coil unit is

$$B = \left|\dot{B}\right| = \sqrt{\left|\dot{B}_x\right|^2 + \left|\dot{B}_y\right|^2 + \left|\dot{B}_z\right|^2} \tag{6}$$

2.2. FBISC Structure

In order to minimize the leakage magnetism of the system in the target region while maintaining a high transmission efficiency, it is necessary to analyze the active coil shielding principle. According to SAEJ2954 on electric vehicle leakage measurement, the leakage magnetic field measurement area should be at a distance of 0.8 m from the center of the charging coil. As shown in Figure 2, this paper defines the measurement area as the target area, which is located at a distance of 800 mm from the center of the coil, and at a height of 700 mm from the ground.

As shown in Figure 3, the target region is exposed to the unweakened leakage radiation from the conventional unipolar coil, which results in a large leakage; as shown in Figure 4, the reverse DD coil splits the unipolar coil into two coils and connects them in series in the reverse direction, and the magnetic potentials of two coils are in opposite directions, which greatly weaken the leakage on the target region. By observing the flux distributions of the conventional coil and the reverse DD coil, it can be seen that the reverse DD coil weakens the flux in the Y direction compared to the conventional coil by the reverse series connection. Based on this principle, this paper proposes a bidirectional inverse series coils of four meshes structure to further reduce the magnetic leakage in the area of the human body's activity range during the charging process of an electric vehicle while maintaining a high transmission efficiency. This structure further divides the reverse DD coil into meshes, which reduces the Y-direction flux in the Y-direction more efficiently while canceling out the X-direction flux as well. As shown in Figure 5, the FBISC structure splits the DD coil into four coils in the observation plane direction.

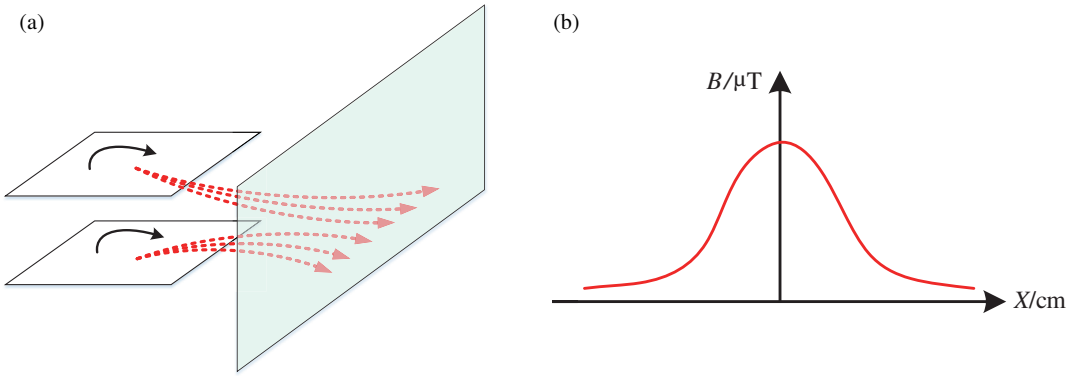

FIGURE 3. Flux distribution of conventional air-core coils. (a) Distribution of magnetic inductance of the air-core coils. (b) Magnetic flux distribution in the target area.

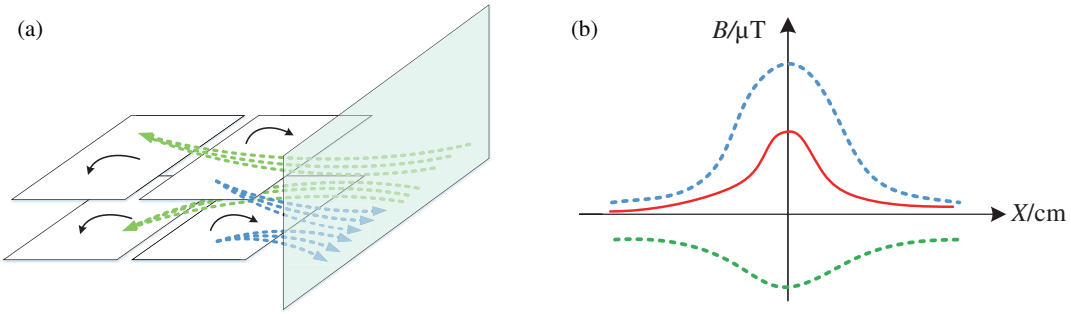

FIGURE 4. Flux distribution of the reverse DD coil. (a) Distribution of magnetic inductance of the reverse DD coil. (b) Magnetic flux distribution in the target area.

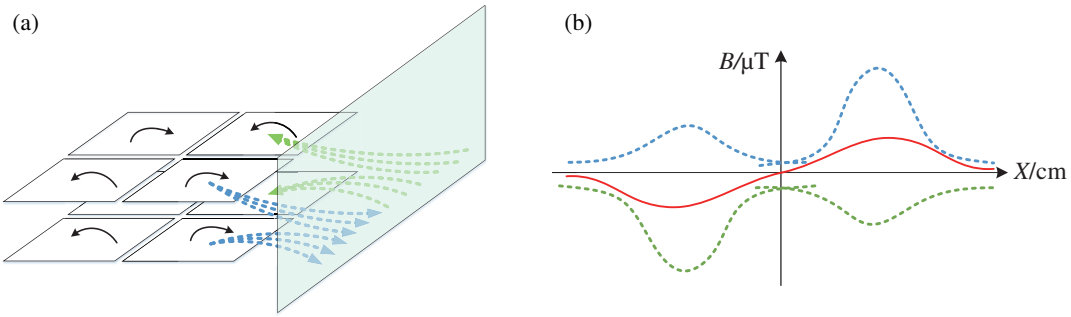

FIGURE 5. Flux distribution of the FBISC coil. (a) Distribution of magnetic inductance of the FBISC coil. (b) Magnetic flux distribution in the target area.

As shown in Figure 1, both the transmitting and receiving coils of the FBISC structure consist of four coil units, each of which is connected in reverse series with the neighboring coils in both the transverse and longitudinal directions. The FBISC structure greatly attenuates the magnetic flux in both the X-direction (the forward direction of the vehicle) and Y-direction (the door-side direction) through the quadruple division of the unipolar coils, which increases the safety index of the leakage radiation of the charging process of the electric vehicle.

According to the structure schematic shown in Figure 1, the equivalent circuit model of the FBISC structure can be obtained, as shown in Figure 6. The FBISC coil structure can be equated to two circuits with coils shown in Figure 7. T_x is the transmitting coil; R_x is the receiving coil; C_1, L_1, and R_1 are the resonant capacitance, self-inductance, and equivalent resistance of the transmitting coil; C_2, L_2, and R_2 are the resonant capacitance, self-inductance, and equivalent resistance of the receiving coil; and M is the mutual inductance of Coil_1 and Coil_2, respectively. Based on the equivalent circuit model the following matrix of Kirchhoff voltage equations can be established.

$$\begin{bmatrix} \dot{Z}_1 & j\omega M \\ j\omega M & \dot{Z}_2 \end{bmatrix} \begin{bmatrix} \dot{I}_{Tx} \\ \dot{I}_{Rx} \end{bmatrix} = \begin{bmatrix} \dot{V}_S \\ 0 \end{bmatrix} \tag{7}$$

Since the structure is in resonance, where impedance $Z_1 = R_1 + R_S$, impedance $Z_2 = R_2 + R_L$, and R_S is the internal resistance of

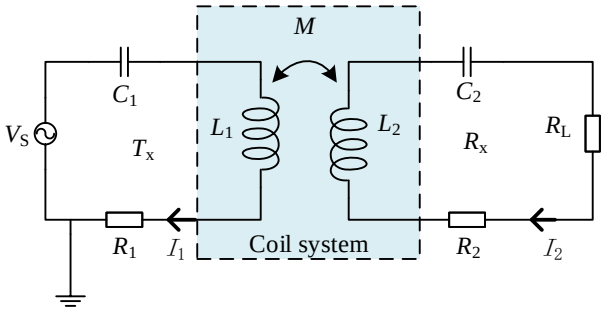

FIGURE 6. Equivalent circuit model of FBISC coil structure.

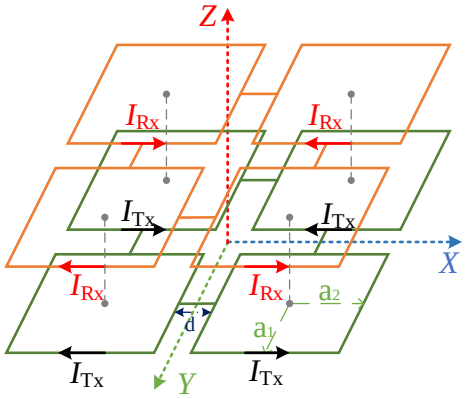

FIGURE 7. Schematic diagram of FBISC structure.

the power supply V_S. The resulting expressions for the currents I_1 and I_2 are given by

$$\begin{cases} \dot{I}_1 = \dfrac{\dot{Z}_2 \dot{V}_S}{\dot{Z}_1 \dot{Z}_2 + (\omega M)^2} \\ \dot{I}_2 = -\dfrac{j\omega M \dot{V}_S}{\dot{Z}_1 \dot{Z}_2 + (\omega M)^2} \end{cases} \tag{8}$$

According to Eq. (8), an expression for the transmission efficiency can be obtained

$$\eta = \left| \frac{\dot{I}_{Rx}^2 R_L}{\dot{V}_S \dot{I}_{Tx}} \right| = \left| -\frac{(\omega M)^2 R_L}{\dot{Z}_1 \dot{Z}_2^2 + (\omega M)^2 \dot{Z}_2} \right| \tag{9}$$

Bringing the impedance values $Z_1 = R_s + R_1$, $Z_2 = R_L + R_2$ into (10), we get

$$\eta = \frac{(\omega M)^2 R_L}{(R_s + R_1)(R_2 + R_L)^2 + (\omega M)^2 (R_2 + R_L)} \tag{10}$$

Based on Equation (10), the derivation of R_L yields the optimal load expression for this structure at maximum transmission efficiency as

$$R_{L\text{opt}} = \sqrt{\frac{(R_s + R_1) R_2^2 + (\omega M)^2 R_2}{(R_s + R_1)}} \tag{11}$$

2.3. Structural Optimization

Figure 7 shows the physical model of the FBISC structure, where the four coil units that make up the transmitting and receiving coils, respectively, have the same length and width parameters, and the distances between neighboring two coils are equal in the transverse and longitudinal directions. Calculation of the magnetic induction strength between the transmitting and receiving coils of the FBISC coil requires the calculation of the magnetic induction strength of each small coil unit, which is then vectorially superimposed. The magnetic induction intensity components in each direction of the eight coil units of the FBISC coil structure are calculated by Equations (3), (4), and (5) to obtain the total magnetic induction intensity components in each direction, and the total magnetic induction intensity is found by Equation (6).

The FBISC structure proposed in this paper aims to maintain a high transmission efficiency of the electric vehicle wireless energy transmission system while reducing the magnetic leakage within the range of human activity. According to the latest EN 62233 test standard issued by the Electrotechnical Standardization Committee (ESC), which states that the value of the magnetic field basically harmless to the human body should be less than 6.25 μT, the following structure optimization process is designed in this paper. Under the premise of determining the coil structure, according to the magnetic induction strength calculation and transmission efficiency calculation method proposed in Subsection 2.1, it can be found that the two important parameters of measuring the structure, the transmission efficiency η and the maximum leakage magnetization $B_{\max}$, are related to the coil inner diameter and the number of turns. Therefore, the following optimization process, which is shown in Figure 8, is designed to seek the optimal parameters while ensuring that the transmission efficiency is higher than 95% and the maximum magnetic leakage in the target region lower than the human body safety value of 6.25 μT. The scope and results of parameter optimization are shown in Table 1.

(1) Parameter initial value setting: the wire selection of 3.96 mm outside diameter Litz copper wire, the composition of the transmitter coil and receiver coil of the eight small coil unit length, width, number of turns are set to a uniform initial value: the inner length of a is set to 20 cm to 28 cm; the step is 1 cm; the inner width of b is set to 12 cm to 18 cm; the step is 1 cm; the number of turns n is set to 10 turns to 20 turns; the step is 1 turn.

(2) Selection of output power and calculation of coil parameters: Considering the actual demand and the existing technology level, the output power is set to 4 kW, and according to Eqs. (7)–(10) and (13), the mutual inductance of the coil M, the optimal load R_L, the receiving current I_2, and the input voltage V_S can be calculated.

(3) Calculate the coil transmission efficiency η and the maximum magnetic leakage of the observation surface $B_{\max}$: The transmission efficiency is obtained by Eqs. (11) and (12); the

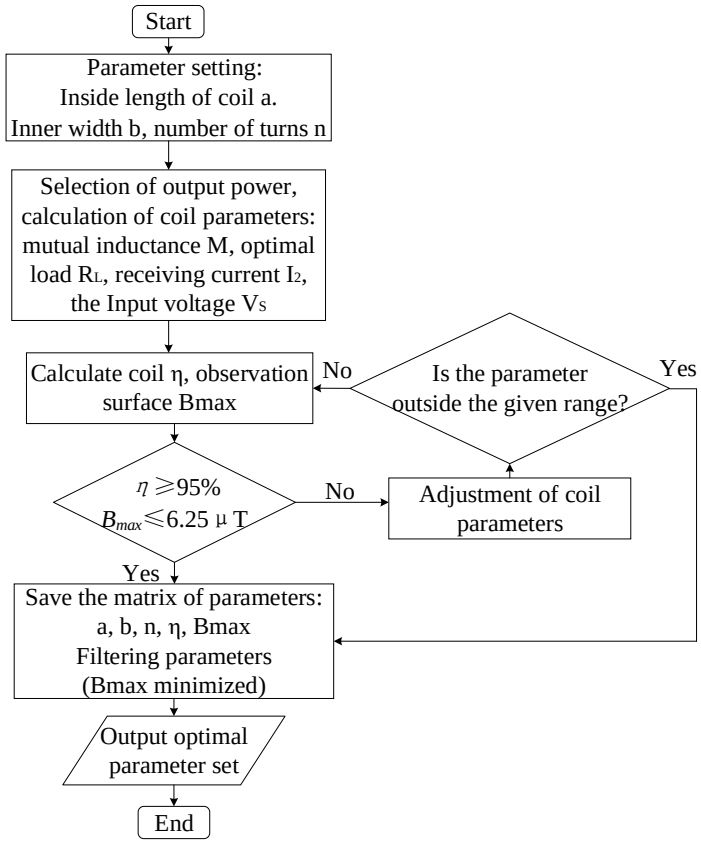

FIGURE 8. Optimization flow chart.

TABLE 1. Optimized parameter ranges and results.

Parameter	Optimization range	Optimization results
a	20 cm–28 cm	24 cm
b	12 cm–18 cm	14 cm
n	10 turns–20 turns	20 turns

range of the target area is set as X-axis (−1000 mm, 1000 mm), Y-axis (700 mm), Z-axis (0 mm, 700 mm); and the distribution of magnetic leakage of the target area and the maximum magnetic leakage coordinates can be obtained in Matlab according to Eqs. (1)–(6).

(4) Data screening: the transmission efficiency obtained for each parameter group is compared and screened against the magnetic leakage, and if $\eta \geq 95\%$ and $B_{\max} \leq 6.25$ μT, the parameter group is retained in the parameter matrix; otherwise, the coil parameters continue to be optimized, and the optimization procedure is ended when the upper limit of the parameter settings is reached, and the process is jumped to the next step.

(5) Output optimal parameters: in order to make the structure achieve better magnetic shielding performance while maintaining high transmission efficiency, the parameter group with the smallest $B_{\max}$ is screened out of the parameter group with $\eta \geq 95\%$ and $B_{\max} \leq 6.25$ μT retained in the previous step, and the parameter group obtained by screening maintains high efficiency and ensures the best shielding effect. The number of parameters output by screening is the optimal parameters obtained by optimization. The final coil parameters obtained are: the inner length a is 24 cm; the inner width b is 14 cm; the number of turns n is 20; and all coil unit parameters are consistent.

3. EXPERIMENTAL VERIFICATION

In this section, in order to validate the proposed and optimized magnetic shielding structure, a set of electric vehicle wireless energy transmission system with shielding is constructed, and the feasibility and correctness of the proposed structure is proved through experimental analysis comparing the proposed structure with the conventional coils, the maximum leakage point leakage of the target area of the inverted DD coils, and the transmission efficiency, which is mutually confirmed from the theoretical calculations, simulations, and experiments. Figure 9(a) shows the WPT experimental bench built in this paper, and Figures 9(b), (c), (d) show the FBISC coil, conventional coil, and DD coil configurations, respectively, which have the

FIGURE 9. Experimental setup. (a) Experimental system diagram. (b) FBISC coil configuration. (c) Conventional coil configuration. (d) DD coil configuration.

same size and number of turns for both their transmitting and receiving coils.

3.1. Experimental Setup

In this section, an experimental platform is set up as shown in Figure 9(a). The electric vehicle wireless energy transmission system used in the experiment consists of a DC source, an inverter module, a wireless energy transmission system, a rectifier module, and a load. The DC power output from the DC source is transferred to the transmitting side of the WPT system through the inverter module, transferred to the receiving side through the wireless transmission, and then flows through the rectifier module to the load. The inverter module and rectifier module both use SiC power devices with a maximum withstand current of 30 A, model C3M0075120D. The WPT system mainly consists of a coil model of the FBISC coil structure, which has a mesh arrangement of the transmitter and receiver poles, and consists of four small coil units, which are connected in series in the longitudinal direction and transverse direction, with the following dimensions: inner length of 24 cm, inner width of 14 cm, and number of turns of 20. The sizes of the four coil units are 24 cm inner length, 14 cm inner width, 20 turns, wound by 0.1 mm $*$ 800 strands of Litz wire with an outer diameter of 3.96 mm. In addition to this the coil model is equipped with a resonant capacitor; the magnetic induction is measured using NF-5035S electromagnetic radiation analyzer; and the transmission efficiency of the system is measured using the WT5000 power analyzer. The physical parameters of the coil are shown in Table 2.

3.2. Magnetic Leakage and Transmission Efficiency of the Proposed Structure

In order to accurately obtain the leakage magnetic field of the FBISC coil structure in the target area, firstly, a mathematical model is built in Matlab platform according to the magnetic induction intensity calculation method for rectangular coils based on vector magnetic potential given in Eqs. (1) to (13). The three-dimensional leakage magnetic field B_c of the FBISC coil structure in the target area at the maximum offset of 100 mm in the direction of Y-axis when the output power is constant at

TABLE 2. Physical parameters of the coils.

Parameter	Physical meaning	Value
L_{Tx}	Self-inductance of transmitting coil	712/μH
L_{Rx}	Self-inductance of receiving coil	714/μH
C_{Tx}	Compensation capacitance of transmitting coil	5/nF
C_{Rx}	Compensation capacitance of receiving coil	5/nF
R_1	Parasitic resistance of transmitting coil	489/mΩ
R_2	Parasitic resistance of receiving coil	490/mΩ
f_0	Operating frequency	85/kHz
R_L	Load	35/Ω

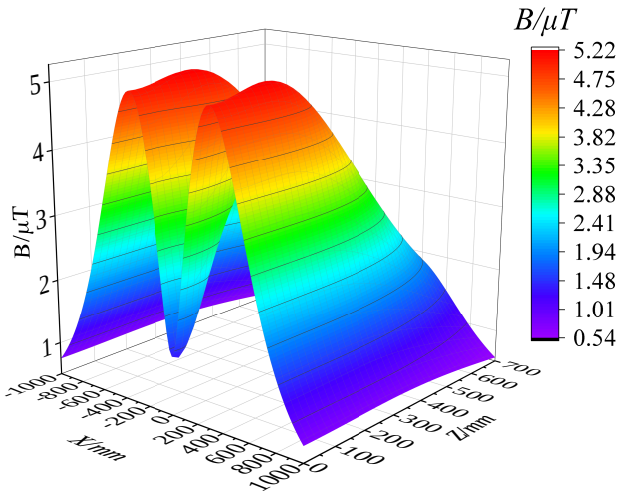

FIGURE 10. Distribution of theoretically calculated values of leakage flux on the target region.

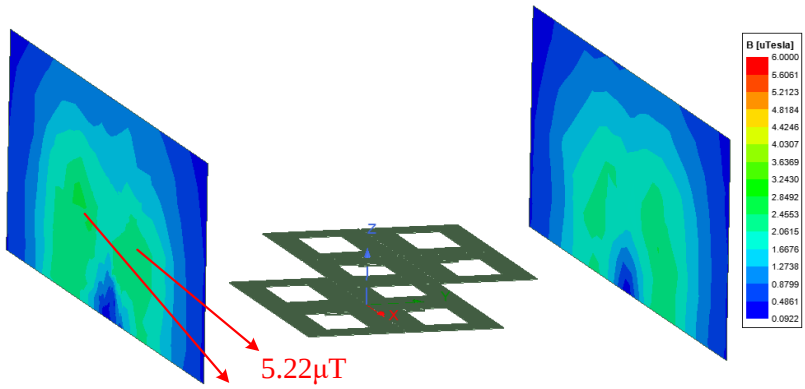

FIGURE 11. Simulation value distribution of leakage flux on the target region.

4 kW is calculated, and the maximum magnetic leakage point of 100 mm in the direction of Y-axis is obtained. The 3D coordinates of the maximum leakage point are obtained, followed by building a simulation model in Ansys Maxwell finite element simulation software, and the maximum leakage field B_s is obtained through system simulation. Finally, the leakage field B_e of the maximum leakage point is measured by using an electromagnetic radiation analyzer, NF-5035S, on the built physical platform.

Figure 10 shows the distribution of the theoretical values of the leakage magnetic field on the observation surface of the FBISC coil structure at the maximum offset of 100 mm. The coordinates of the maximum leakage point are (−300 mm, 800 mm, 160 mm), (300 mm, 800 mm, 160 mm), and the maximum leakage flux is 5.22 μT. The simulation model is built in Ansys Maxwell as shown in Figure 11, and the maximum leakage flux obtained is B_s. The magnitude of the maximum leakage magnetic field in the target region at an offset of 0–100 mm

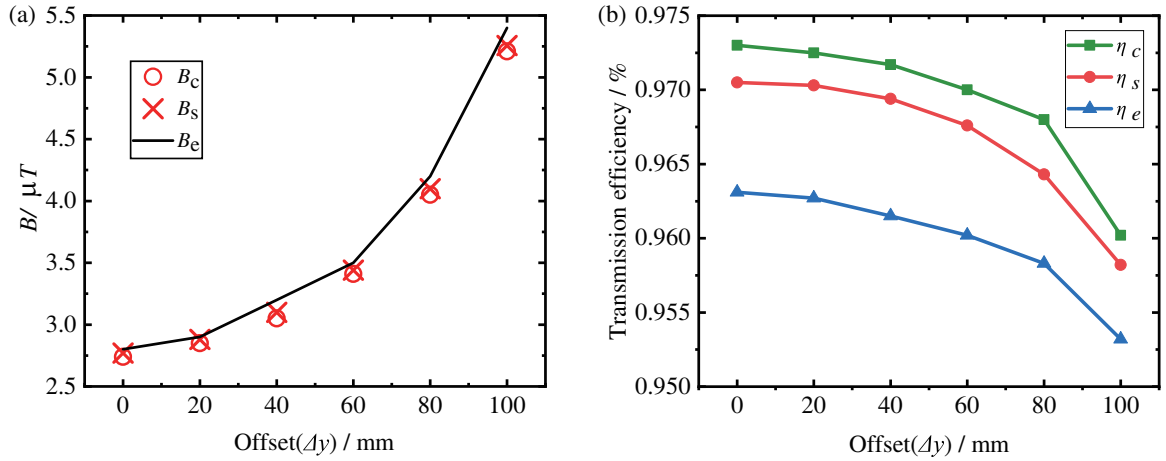

FIGURE 12. Leakage magnetic field and efficiency of FBISC structure at different offset distances. (a) Leakage magnetic field of FBISC coil structure. (b) Transmission efficiency of FBISC structure system.

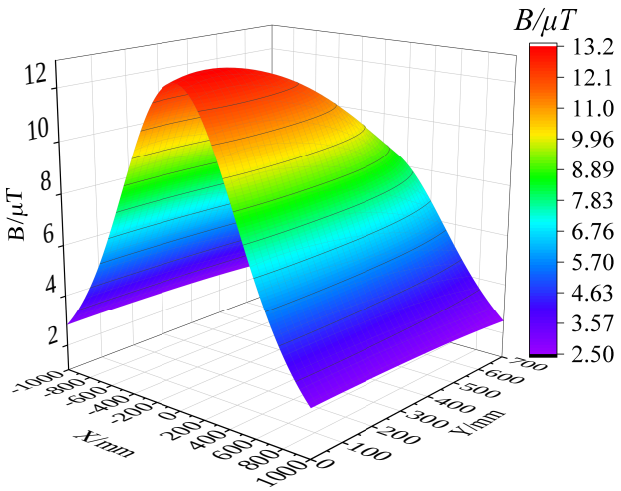

FIGURE 13. Theoretical value distribution of magnetic leakage of conventional coils on the target region.

of the receiver coil was recorded. Figure 10 shows the simulation model at an offset of 100 mm with a maximum leakage magnetic field of 5.257 μT in the target region. Finally, based on the built electric vehicle wireless energy transmission system with shielding, the measured leakage flux of the FBISC coil structure at the maximum leakage point at the observation surface is measured using the NF-5035S electromagnetic radiation analyzer.

Figure 12(a) demonstrates the theoretically calculated, simulated, and experimental values of the leakage magnetic field of the FBISC coil structure at offsets of 0–100 mm. It is observed that the error in the theoretically calculated, simulated, and measured values at each offset remains below 7%.

Figure 12(b) shows the system transmission efficiency of the FBISC coil structure system at offsets from 0 to 100 mm. The transmission efficiency of this structure is higher than 95% at all offsets from 0 to 100 mm and decreases with increasing offset distance.

3.3. Magnetic Leakage and Transmission Efficiency of Conventional Coil

Figure 13 shows the distribution of theoretical values on the target area of the conventional rectangular coil at the maximum offset of 100 mm. It can be seen that the leakage magnetic field at the maximum leakage point is 13.2 μT.

Figure 14 shows the distribution of the leakage simulation values of the conventional rectangular coil on the target region at the maximum offset of 100 mm, and the maximum leakage magnetization in the target area is 13.1 μT. The leakage field is mainly distributed between the transmitting coil and receiving coil, which is consistent with the distribution of the leakage field in Figure 13.

Figure 15(a) shows the theoretically calculated, simulated, and experimental values of the leakage magnetic field of the traditional rectangular coil at an offset of 0–100 mm. The error in the theoretically calculated, simulated, and experimental values is less than 5% at each offset.

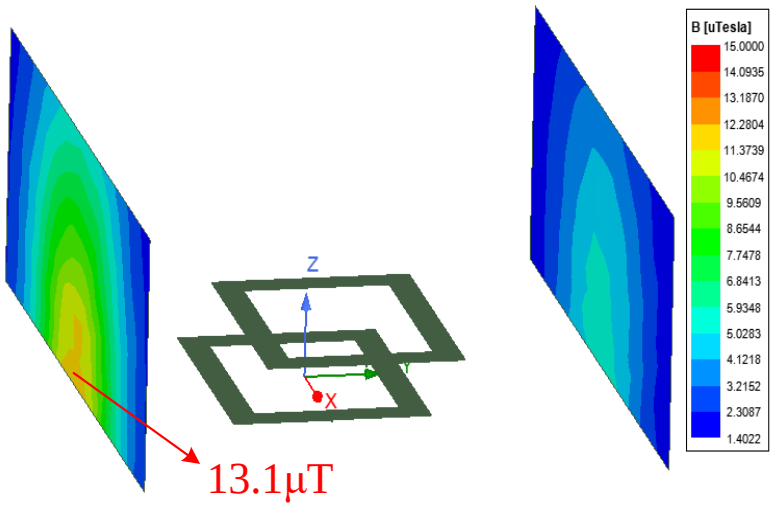

FIGURE 14. Simulated value distribution of magnetic leakage of conventional coil on the target region.

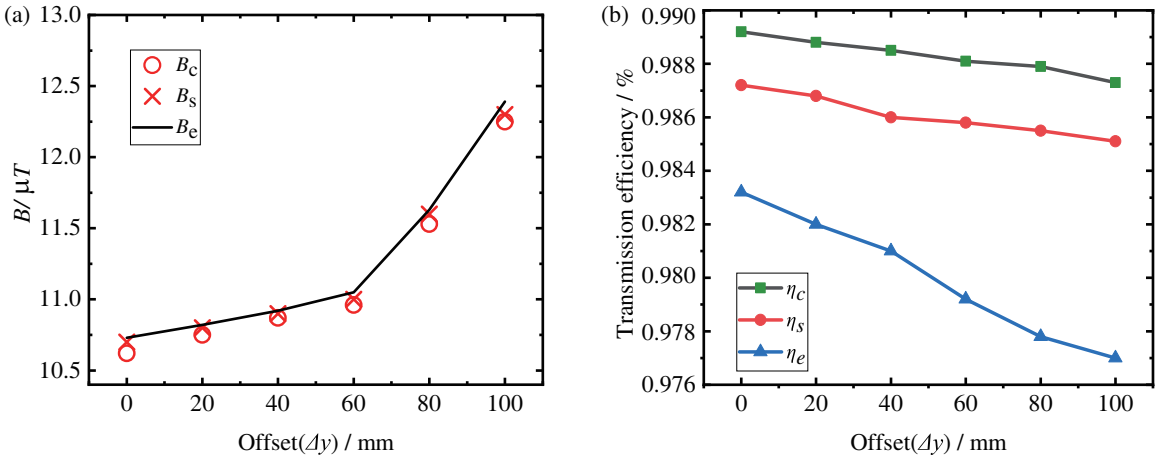

FIGURE 15. Leakage magnetic field and efficiency of conventional coils at different offset distances.

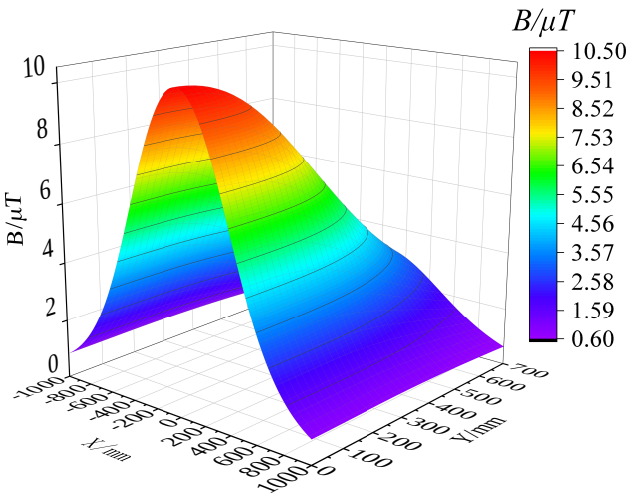

FIGURE 16. Theoretical value distribution of magnetic leakage of reverse DD coil on the target region.

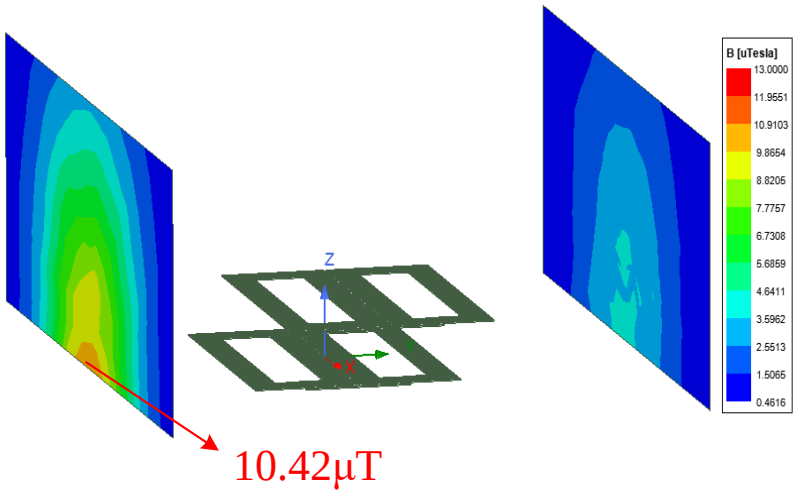

FIGURE 17. Simulated value distribution of leakage flux on the target region for reverse DD coil.

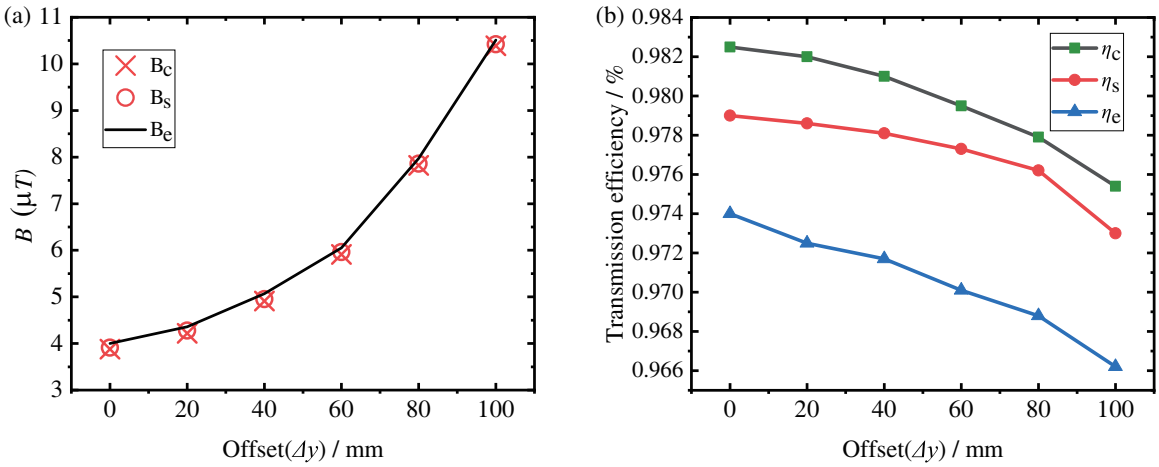

FIGURE 18. Leakage magnetic field and efficiency of conventional coils at different offset distances. (a) Leakage magnetic field of the inverted DD coil. (b) Transmission efficiency of the reverse DD coil system.

Figure 15(b) shows the system transmission efficiency of conventional coil system at offset 0–100 mm. The efficiency of this structure is higher than 95% at all offsets from 0 to 100 mm and decreases with increasing offset distance. Through this subsection, it can be seen that the FBISC structure proposed in this paper reduces the leakage magnetic field by 56.4% compared to the conventional coil with the same outer diameter and maintains a transmission efficiency higher than 95% while sacrificing only 2.38% transmission efficiency.

3.4. Magnetic Leakage and Transmission Efficiency of Reverse DD Coil

Figure 16 shows the theoretical value distribution of the reverse DD coil on the observation surface at the maximum offset of 100 mm. It can be seen that the magnitude of leakage flux at the maximum leakage point is 10.5 μT.

Figure 17 shows the distribution of the leakage simulation value of the conventional rectangular coil on the target region at the maximum offset of 100 mm, and the maximum leakage magnetization in the target area is 10.42 μT. The leakage magnetic field is mainly distributed near the transmitting coil, which is consistent with the distribution of the leakage magnetic field in Figure 16.

Figure 18(a) shows the theoretically calculated, simulated, and experimental values of the leakage magnetic field of the traditional rectangular coil at an offset of 0–100 mm. The error of the theoretically calculated, simulated, and experimental values is less than 5% at each offset.

Figure 18(b) shows the system transmission efficiency of the reverse DD coil system at offset 0–100 mm. The efficiency of this structure is higher than 95% at all offsets from 0 to 100 mm and decreases with increasing offset distance Through this subsection, it can be seen that the FBISC structure proposed in this paper reduces the leakage flux by 48.5% compared to conven-

TABLE 3. Performance comparison table.

Documentary sources	Shielding methods	Shielding efficiency	Transmission efficiency
[18]	Reactive resonance shielding	30.8%	/
[20]	Without source coils	45%	70%
[25]	Source coils	51%	92.8%
This paper	Source coils	56.4%	96.31%

tional coils with the same outer diameter and maintains a high transmission efficiency at the same time.

3.5. Performance Comparison

This subsection compares the shielding method proposed in this paper with other studies. It includes shielding method, shielding efficiency, and transmission efficiency. The results are shown in Table 3. It shows that the structure proposed in this paper has good magnetic shielding performance and transmission efficiency.

4. CONCLUSION

In this paper, a bidirectional inverse series coils of four meshes coil structure is proposed, which greatly reduces the leakage magnetic field in the target region while maintaining high transmission efficiency. The structure is characterized by splitting the transmitting and receiving coils into four meshes, and the four small meshes units are connected in reverse series with each other, so that when the current passes through, the current direction of the adjacent coils is reversed, and the leakage magnetic field around the electric vehicle during charging is shielded by this structure. In addition, a coil parameter optimization method is proposed, in which the optimal parameters of the coil that satisfy the conditions are obtained by setting the target values for the dual optimization objectives (magnetic leakage and transmission efficiency). Finally, a physical experimental platform is built based on the optimal parameters, and it is found that the FBISC coil structure reduces the leakage magnetic field in the target area by 56.4% and 48.5% compared with the conventional unipolar and DD coils, respectively, at the maximum offset of 100 mm, and at the same time maintains more than 95% of the transmission efficiency. It can be seen that the FBISC coil structure has higher safety and practicability for the electric vehicle wireless energy transmission system, and future research should tend to simplify the structure, reduce the material, and lower the cost of use while ensuring the human body safety and the transmission efficiency of the system.

ACKNOWLEDGEMENT

This work was supported in part by the Natural Science Foundation of Hunan Province under Grants 2022JJ30226 and in part by the National Key R&D Program Project (2022YFB3403200) and in part by Key Projects of Hunan Provincial Department of Education (23A0432).

REFERENCES

[1] Rituraj, G. and P. Kumar, "A new magnetic structure of unipolar rectangular coils in WPT systems to minimize the ferrite volume while maintaining maximum coupling," *IEEE Transactions on Circuits and Systems II: Express Briefs*, Vol. 68, No. 6, 2072–2076, Jun. 2021.

[2] Hsieh, Y.-C., Z.-R. Lin, M.-C. Chen, H.-C. Hsieh, Y.-C. Liu, and H.-J. Chiu, "High-efficiency wireless power transfer system for electric vehicle applications," *IEEE Transactions on Circuits and Systems II: Express Briefs*, Vol. 64, No. 8, 942–946, Aug. 2017.

[3] Popović-Gerber, J., J. A. Oliver, N. Cordero, T. Harder, J. A. Cobos, M. Hayes, S. C. O'Mathuna, and E. Prem, "Power electronics enabling efficient energy usage: Energy savings potential and technological challenges," *IEEE Transactions on Power Electronics*, Vol. 27, No. 5, 2338–2353, May 2012.

[4] Rituraj, G., B. K. Kushwaha, and P. Kumar, "A unipolar coil arrangement method for improving the coupling coefficient without ferrite material in wireless power transfer systems," *IEEE Transactions on Transportation Electrification*, Vol. 6, No. 2, 497–509, Jun. 2020.

[5] Chen, C., X. Huang, L. Tan, F. Wen, and W. Wang, "Electromagnetic environment and security evaluation for wireless charging of electric vehicles," *Transactions of China Electrotechnical Society*, Vol. 30, No. 19, 61–67, 2015.

[6] Dong, L., F. H. Lin, C. Q. Wang, *et al.*, "Assessing human exposure to electromagnetic fields from catenary-freepower supply urban rail transit vehicle," *Transactions of China Electrotechnical Society*, Vol. 36, No. S1, 40–45, 2021.

[7] Gaona, D. E., S. Ghosh, and T. Long, "Feasibility study of nanocrystalline-ribbon cores for polarized inductive power transfer pads," *IEEE Transactions on Power Electronics*, Vol. 35, No. 7, 6799–6809, Jul. 2020.

[8] Zhang, W., Q. Yang, Y. Li, Z. Lin, M. Yang, and M. Mi, "Comprehensive analysis of nanocrystalline ribbon cores in high-power-density wireless power transfer pads for electric vehicles," *IEEE Transactions on Magnetics*, Vol. 58, No. 2, 8700605, Feb. 2022.

[9] Zhang, P., Q. Yang, X. Zhang, Y. Li, and Y. Li, "Comparative study of metal obstacle variations in disturbing wireless power transmission system," *IEEE Transactions on Magnetics*, Vol. 53, No. 6, 9100304, Jun. 2017.

[10] Zhu, Q., D. Chen, L. Wang, C. Liao, and Y. Guo, "Study on the magnetic field and shielding technique for an electric vehicle oriented wireless charging system," *Transactions of China Electrotechnical Society*, Vol. 30, No. S1, 143–147, 2015.

[11] Fan, X., H. Zhang, F. Tang, *et al.*, "Investigation and application of electromagnetic metamaterials in the field of wireless power transfer," *Proceedings of the CSEE*, 1–19, 2022.

[12] Tian, Z., J. Chen, J. Fan, *et al.*, "The wireless power transfer system with magnetic metamaterials," *Transactions of China Electrotechnical Society*, Vol. 30, No. 12, 1–11, 2015.

[13] Das, R., A. Basir, and H. Yoo, "A metamaterial-coupled wireless power transfer system based on cubic high-dielectric resonators," *IEEE Transactions on Industrial Electronics*, Vol. 66, No. 9, 7397–7406, Sep. 2019.

[14] Lu, C., X. Huang, C. Rong, X. Tao, Y. Zeng, and M. Liu, "A dual-band negative permeability and near-zero permeability metamaterials for wireless power transfer system," *IEEE Transactions on Industrial Electronics*, Vol. 68, No. 8, 7072–7082, Aug. 2021.

[15] Shaw, T. and D. Mitra, "Wireless power transfer system based on magnetic dipole coupling with high permittivity metamaterials," *IEEE Antennas and Wireless Propagation Letters*, Vol. 18, No. 9, 1823–1827, Sep. 2019.

[16] Lu, C., C. Rong, X. Huang, Z. Hu, X. Tao, S. Wang, J. Chen, and M. Liu, "Investigation of negative and near-zero permeability metamaterials for increased efficiency and reduced electromagnetic field leakage in a wireless power transfer system," *IEEE Transactions on Electromagnetic Compatibility*, Vol. 61, No. 5, 1438–1446, 2019.

[17] Kim, J., J. Kim, S. Kong, H. Kim, I.-S. Suh, N. P. Suh, D.-H. Cho, J. Kim, and S. Ahn, "Coil design and shielding methods for a magnetic resonant wireless power transfer system," *Proceedings of the IEEE*, Vol. 101, No. 6, 1332–1342, 2013.

[18] Kim, S., H.-H. Park, J. Kim, J. Kim, and S. Ahn, "Design and analysis of a resonant reactive shield for a wireless power electric vehicle," *IEEE Transactions on Microwave Theory and Techniques*, Vol. 62, No. 4, 1057–1066, 2014.

[19] Moon, H., S. Kim, H. H. Park, and S. Ahn, "Design of a resonant reactive shield with double coils and a phase shifter for wireless charging of electric vehicles," *IEEE Transactions on Magnetics*, Vol. 51, No. 3, 8700104, 2015.

[20] Kim, J., J. Kim, S. Kong, H. Kim, I.-S. Suh, N. P. Suh, D.-H. Cho, J. Kim, and S. Ahn, "Coil design and shielding methods for a magnetic resonant wireless power transfer system," *Proceedings of the IEEE*, Vol. 101, No. 6, 1332–1342, 2013.

[21] Mi, M., Q. Yang, Y. Li, P. Zhang, and W. Zhang, "Multi-objective active shielding coil design for wireless electric vehicle charging system," *IEEE Transactions on Magnetics*, Vol. 58, No. 2, 8700505, 2022.

[22] Lee, S., D.-H. Kim, Y. Cho, H. Kim, C. Song, S. Jeong, J. Song, G. Park, S. Hong, J. Park *et al.*, "Low leakage electromagnetic field level and high efficiency using a novel hybrid loop-array design for wireless high power transfer system," *IEEE Transactions on Industrial Electronics*, Vol. 66, No. 6, 4356–4367, 2019.

[23] Li, Z., P. Kong, L. Ren, X. Xiong, J. Li, W. Wu, and H. Liu, "Leakage magnetic field calculation and optimization of double inverse series coil structure of electric vehicle wireless charging systems," *Progress In Electromagnetics Research B*, Vol. 96, 213–233, 2022.

[24] Li, Z. Q., J. Li, C. H. Quan, X. Y. Zhang, S. D. Huang, *et al.*, "Mutual inductance calculation of arbitrarily positioned rectangular coils with magnetic shielding in wireless power transfer systems," *Transaction of China Electrotechnical Society*, 1–12, 2022.

[25] Mi, M., Q. Yang, Y. Li, P. Zhang, and W. Zhang, "Multi-objective active shielding coil design for wireless electric vehicle charging system," *IEEE Transactions on Magnetics*, Vol. 58, No. 2, 8700505, Feb. 2022.